DFT Study on the Compatibility Between Bentonite Clay Mineral and Hydration Products With the Polycarboxylate Water Reducer in the Cement Hydration Process

Huang Teng[1,2], Zhihao He[3,4,5]*, Gao Meiben[5] and Jiaxing Zhang[3,4]

[1]Key Laboratory of Solid Waste Treatment and Resource Recycle Ministry of Education, Southwest University of Science and Technology, Mianyang, China, [2]School of Environment and Resource, Southwest University of Science and Technology, Mianyang, China, [3]State Key Laboratory of Geohazard Prevention and Geoenvironment Protection, Chengdu University of Technology, Chengdu, China, [4]College of Environmental and Civil Engineering, Chengdu University of Technology, Chengdu, China, [5]School of Emergency Management, Xihua University, Chengdu, China

As one of the most used grouting materials, cement has the characteristics of low price and a wide resource of raw material. With the in-depth research and application of cement admixture, the compatibility between different water-reducing agents and clay has become one of the critical factors that affects the cement hydration process. Due to the adsorption of clay on cement additives, the dispersion efficiency of the water reducer will be reduced, also the strength and impermeability of hydration products will be adversely affected. This paper studies the adsorption characteristics of different PCE superplasticizers on bentonite clay minerals and hydration products using a molecular simulation technique. Results showed that there is competitive adsorption between the clay and hydration products when the admixture participates in the hydration reaction, the additives are likely to adsorb on the CH rather than the clay minerals, while the adsorption energy of the hydration product C-S-H is the highest, thus the preferential adsorption order and compatibility between clay minerals and hydration products on admixtures could also be obtained. PDOS (partial density of states) analysis concluded that some new characteristic peaks and rearrangement of the bonding orbitals may appear after the adsorption, with the peak value of the minerals higher than that of jennite, which is also consistent with the adsorption energy. This study aims to reveal the interaction mechanism and compatibility between the hydration product and clay minerals, hoping to fully utilize the advantages of both clay minerals and admixtures in the cement hydration process.

Keywords: geological disasters, grouting material, cement hydration, bentonite, compatibility, DFT

1 INTRODUCTION

With the rapid development of various engineering construction methods, unfavorable geological conditions, such as joints and fracture zones with dense fissures and water-saturated fissures, are often exposed in engineering activities, resulting in geological disasters such as instability and damage of the slope and surrounding rock, threatening engineering construction and safe operation.

For the prevention and control of the above rock mass cracks and water inrush disasters, the grouting method is usually used for plugging and reinforcement. As one of the most used grouting materials, cement has the characteristics of low price and a wide resource of raw material. Due to the environmental pollution caused by the production process, there is an urgent need to seek similar environmentally friendly substitute materials. Adding a certain amount of clay minerals into the cement slurry may be conducive to improve the stone strength and injectability of the slurry (Jae et al., 2014; Sharma et al., 2021), while admixtures in cement hydration could also effectively adjust or improve the hydration time and mechanical properties, which may possess advantages of small dosage and low cost (Wang, 2013).

With the in-depth research and application of cement hydration admixtures, the compatibility between additives, such as the polycarboxylate superplasticizer, and clay minerals has also become a key factor in the performance of cement slurry (Tregger et al., 2010; Nathan et al., 2010; Jae et al., 2014). As clay will compete with cement to adsorb the polycarboxylate superplasticizer at the same time, there may be an adverse effect on the strength, wearability, and pourability of the hydration products (Norvell et al., 2007; Pardal et al., 2009; Ng and Plank, 2012). Wang et al. (2013) studied that the adsorption capacity of montmorillonite on the polycarboxylate superplasticizer is much greater than that of the cement, so the dispersion ability on the polycarboxylate superplasticizer may decrease obviously. Lei et al. (2012) also studied the interaction between sodium bentonite and the polycarboxylate superplasticizer, and found that the adsorption form in clay minerals varied with the difference of admixture concentration. When the concentration of admixture is relatively large, the polycarboxylate superplasticizer will mainly adsorb between the layers of clay minerals.

Most of the existing studies mainly focus on macroscopic experiments with different polycarboxylate superplasticizers (Hu, 2013; Roig-Flores et al., 2021; Wang, 2013). By characterizing the TOC (total organic carbon) value of the water reducer before and after adsorption, the adsorption capacity of clay minerals will be further estimated. While research on the interaction mechanism between clay minerals and polycarboxylate superplasticizers is limited, the influential rule of different mineral compositions on the performance of a water reducer still lacks recognition. With the rapid development of computer technology, the research of molecular simulation in the performance and structural design of cement also shows unique advantages, which could obtain various physical and chemical properties of the molecular system, and can also explore the chemical reaction path, transition state, and reaction mechanism from the electronic level. Jingming et al. (2009) investigated the molecular environment and the alkyl chain arrangement in the interlayer of cation surfactant-modified montmorillonite using the molecular simulation technique, and the influence caused by water content in organic montmorillonite with different surfactant loading concentrations was also studied. By building the adsorption model using the molecular simulation, our team's previous studies found that the adsorption energy of hydration product $Ca(OH)_2(CH)$ with different functional groups will be varied, the order of the adsorption energy is sulfonic group > carboxyl group > amide group > benzene ring; the ratio of hydroxyl group and carboxyl group will also affect the adsorption energy on CH (Zhang et al., 2021a; He, 2022).

So based on our previous studies, bentonite clay mineral has been taken as the research object in the text. Combined with the cognition on the adsorption characteristic between the mineral composition of bentonite and different water reducers, we will then further reveal the discrepancy of adsorption energy and the interaction mechanism on different hydration products, so the preferential adsorption order and compatibility in cement hydration will be explored (Li et al., 2005; Chen et al., 2017; Zhang J et al., 2017).

2 MODELS AND CALCULATION METHODS

As an important material in cement hydration products, calcium silicate hydrate (C-S-H) typically accounts for 60%–70% of the whole hydration product. For the complexity and amorphism of the C-S-H structure, Taylor considered that C-S-H gel is a highly deformed tobermorite/jennite-like structure. Bonaccorsi et al. (2004) also studied the crystal structures of tobermorite and summarized the molecular models with three different layer spacing: 9, 11, and 14 Å. In many cases, tobermorite, and jennite crystals are used to replace C-S-H gel (Muralidharan et al., 2005; Jeffrey et al., 2011; Vidmer et al., 2014; Yan, 2017). In order to simplify the calculation in this article, we will then take the jennite as the model of cement hydration product C-S-H, with the molecular formula $Ca_9Si_6O_{18}(OH)_6·8(H_2O)$ (Churakov, 2008; Muralidharan et al., 2005).

2.1 Calculation Methods and Parameter Design

Molecular simulation methods mainly contain quantum mechanics (QM) and classical mechanics methods. As a method of quantum mechanics, density functional theory (DFT) has been widely used in material synthesis and surface adsorption. The chemical reaction usually occurs when different molecules collide with each other, and are then adsorbed on the surface. Therefore, the complexity and possibility of the reaction can be further judged through the structure models and calculations of the adsorption energy (Chen and Ye, 2010; Wu et al., 2018). In this study, the surface models of the clay minerals, hydration products, and the adsorption behavior were established based on the DFT method, while the calculation was carried out by Dmol[3] modules in Material Studio (MS). The equilibrium configuration at the lowest energy was determined by geometry optimization using the Becke-Perdew (BP) correction approximation under the generalized gradient approximation (GGA), which can further investigate the variation rules of the adsorption energy and surface charge distribution. The calculation accuracy was set as fine, unless otherwise specified, and the smearing value was set as 0.005 (Wu, et al., 2018; Babaei, et al., 2020; Orazi, et al., 2020; Xing et al., 2020).

FIGURE 1 | Models of the different crystal planes for the clay minerals adopted in the text.
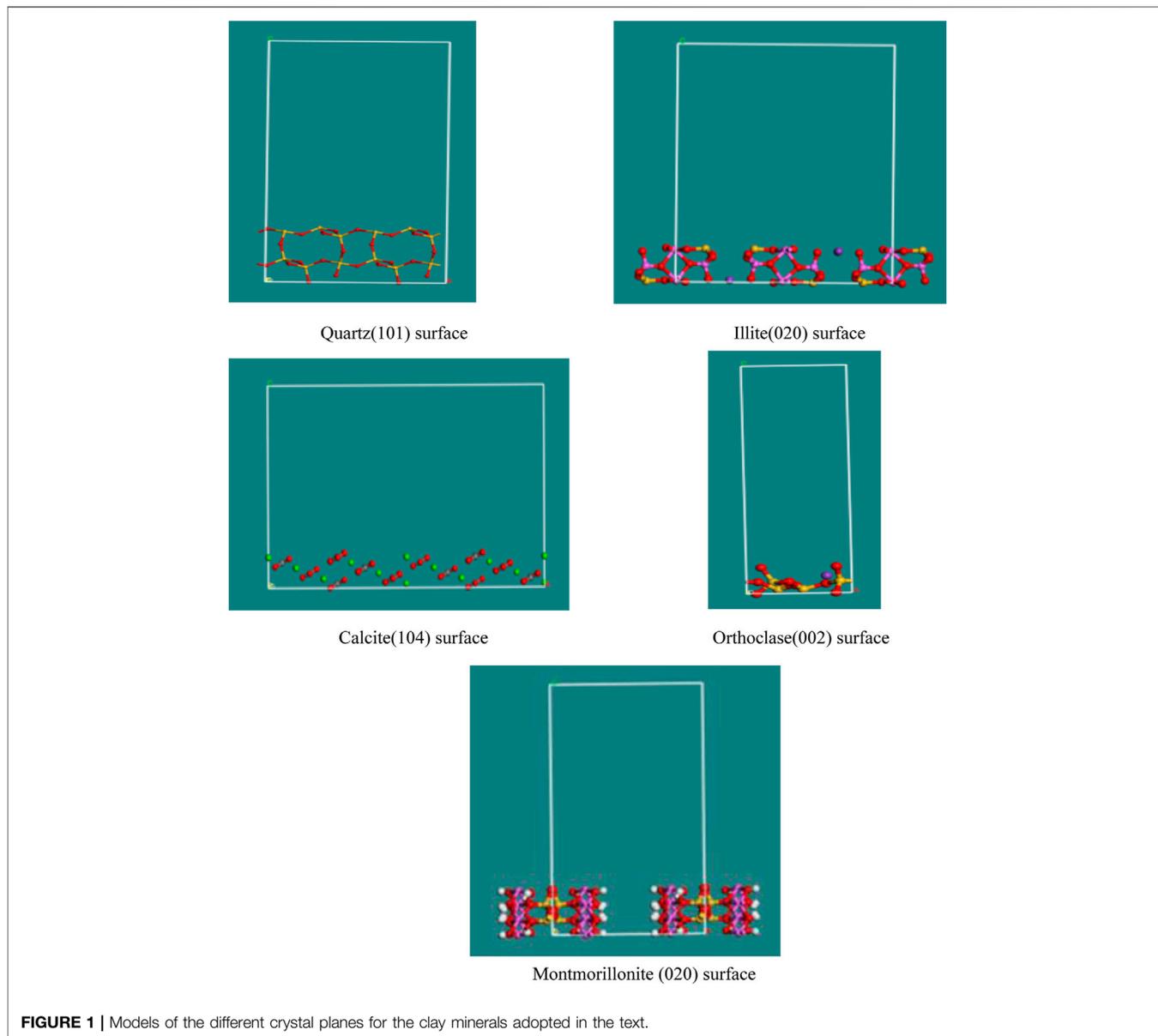
The adsorption energies between the admixtures and clay minerals or the hydration products were calculated as:

$$E_{ads} = E_{total\,(admixtures\,on\,clay)} - E_{admixtures} - E_{clay} \quad (1)$$

$$E_{ads} = E_{total\,(admixtures\,on\,hydration\,products)} - E_{admixtures} - E_{hydration\,products} \quad (2)$$

where E_{ads} is the adsorption energy, $E_{admixtures\,on\,clay}$ and $E_{admixtures\,on\,hydration\,products}$ are the total energy after surface adsorption on the clay minerals or the hydration products, $E_{admixtures}$, E_{clay}, and $E_{hydration\,products}$ are the energies of different admixtures and the minerals before the adsorption. For cases with low adsorption energy, the absorbability is more likely to occur (Zhang S et al., 2017; Bao et al., 2018).

2.2 Calculation Models

Montmorillonite is the main mineral composition of bentonite, and due to the different origins of natural bentonite, the types and content of impurities, such as quartz, calcite, and illite, may be varied. So this study will then focus on the competitive adsorption of the additives between the bentonite clay minerals and the hydration products (Wang et al., 2014; Ko and Kang, 2016; Han et al., 2019).
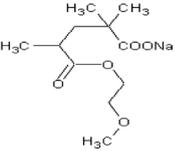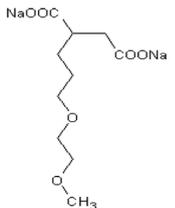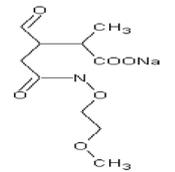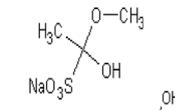
Molecular structure models of different minerals were adopted as shown in **Figure 1**.

According to our previous studies, taking the crystal plane corresponding to the maximum XRD diffraction peak of the single mineral, the crystal planes will also be geometrically optimized by Dmol[3] modules (He, 2022). The energy of

TABLE 1 | Calculation results for the total energy of different minerals after geometry optimization.

Composition	Total energy after geometric optimization/*Ha*
Quartz (101) surface	−5282.5567855
Illite (020) surface	−6105.745843
Calcite (104) surface	−11300.8164968
Orthoclase (002) surface	−4872.0182861
Montmorillonite (020) surface	−6826.1044255

TABLE 2 | Typical functional groups and molecular structures adopted in the text.

	Typical functional group	Molecular structure
(a)	-COOMe, -CH_2-O-CH_2-	
(b)	-COOMe, -CH_2-O-CH_2-	
(c)	-COOMe, -CONH_2, -CH_2-O-CH_2-	
(d)	-SO_3Me	
(e)	-OH, -COOH,	Sodium tartrate
(f)	-OH, -COOH,	Sodium citrate ( )
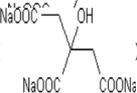
different lattice planes after geometric optimization is shown in **Table 1**.

Admixtures could improve the flow characteristics in the process of cement hydration by dispersion and lubrication. The adsorptive action of the polycarboxylate superplasticizer is mainly due to functional groups such as the hydroxyl group (-OH), carboxyl group (-COO$^-$), sulfonic acid group (-SO$_3^-$), etc., while the length and the density of the side chain could also directly affect the dispersing effect (Yan et al., 2017; Yinwen et al., 2014; Zhang et al., 2021b). Based on our previous studies, taking the functional groups or structural composition of different admixtures as shown in **Table 2**, the adsorption characteristics between the admixtures and the clay minerals will then be explored. For the polycarboxylate superplasticizer involved in this paper, we took a polymerization degree of $n = 1$ as an example (He, 2022).

3 RESULTS AND DISCUSSION

3.1 Adsorption Models of Different Minerals on the Bentonite

3.1.1 Comparison of Adsorption Energy

Clay minerals often contain different impurities, which may reflect the difference in the impact of the hydration process and the properties of hydration products. The adsorption energy of different hydration admixtures on the hydration product CH has been calculated from our previous research, among which sodium tartrate is the lowest (He, 2022). So for sodium tartrate, the comparison of the adsorption energy of different bentonite minerals is presented in **Table 3**.

The adsorption energy is −11.36 eV in montmorillonite, lower than that in other minerals, so the admixtures may be easier to adsorb on the montmorillonite, while the adsorption sequence of different minerals is as follows: montmorillonite > illite > calcite > orthoclase > quartz, which may illustrate that there is competitive adsorption between the clay minerals and hydration products when the admixture sodium tartrate participates in the hydration reaction.

3.1.2 PDOS of Different Minerals Before and After the Adsorption

Based on the molecular dynamics simulation, the total density of states (TDOS) and partial density of states (PDOS) could conduce to obtain more interaction properties and mechanisms of the system, such as electronic structures, tunneling spectroscopy, etc. (Babaei et al., 2020; Xing et al., 2020; Zhang et al., 2015).

Comparison of illite before and after the adsorption with sodium tartrate is presented in **Figure 2**, the sum of the bonding orbital was mainly attributed to the *s* or *p* orbitals, while the *d* and *f* orbitals had little effect on the bond formation. Specifically, the bonding orbital was mainly provided by the *s*

TABLE 3 | Calculation results of the adsorption energy between different minerals of bentonite and sodium tartrate (1 Ha = 27.2114 eV).

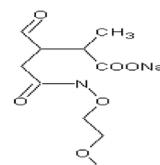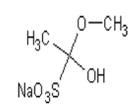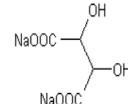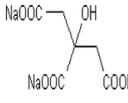|	Sodium tartrate	E_total (Ha)	E_ads (Ha)	E_ads (eV)
Compositions	Quartz (101) surface	−6213.5326	−0.0657	−1.7873
	Illite (020) surface	−7037.0253	−0.3693	−10.0494
	Calcite (104) surface	−12232.0567	−0.3300	−8.9808
	Orthoclase (002) surface	−5803.2234	−0.2950	−8.0271
	Montmorillonite (020) surface	**−7757.4321**	**−0.4175**	**−11.3613**
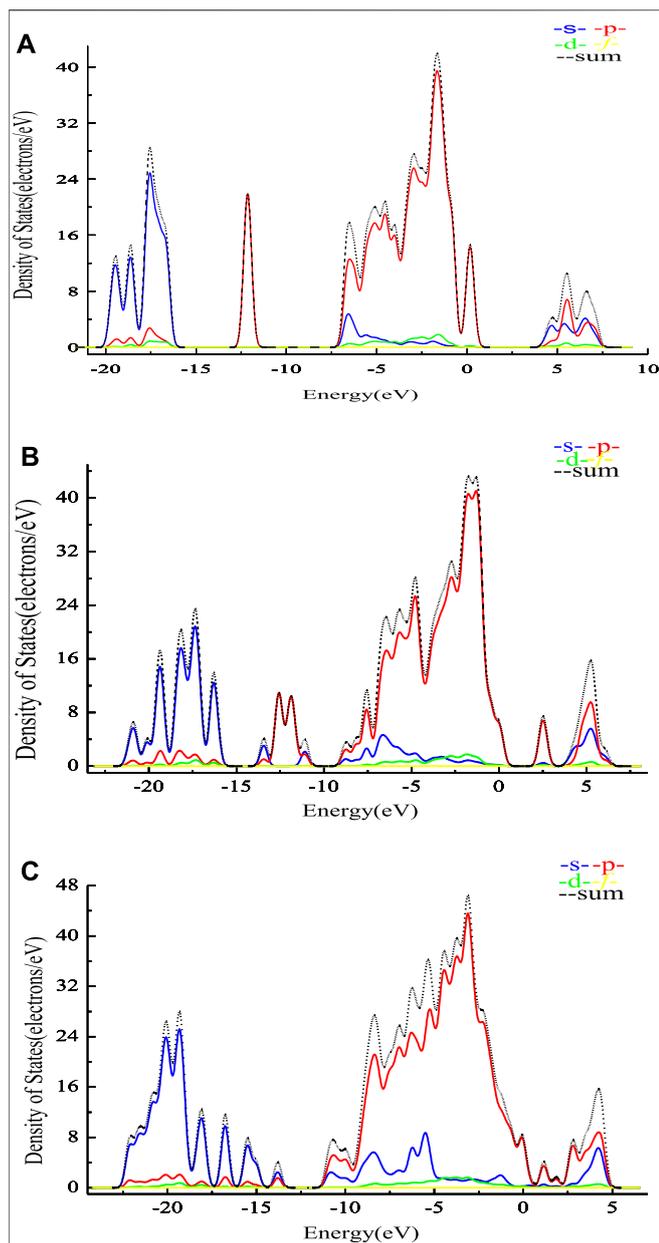
FIGURE 2 | PDOS of different minerals before and after the adsorption. (A) PDOS analysis of the illite (020) surface before adsorption. (B) PDOS analysis between the illite (020) surface and sodium tartrate. (C) PDOS analysis between the montmorillonite (020) surface and sodium tartrate.

TABLE 4 | Calculations of the adsorption energy between the different additives and montmorillonite.

Functional group	Montmorillonite (020) surface	
	E_{ads}/Ha	E_{ads}/eV
(a)	0.2219	6.0383
(b)	−0.1438	−3.9126
(c)	0.2345	6.3801
(d)	**−0.4175**	**−11.3613**
(e)	−0.2467	−6.7133
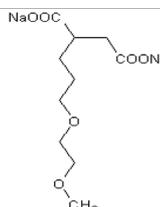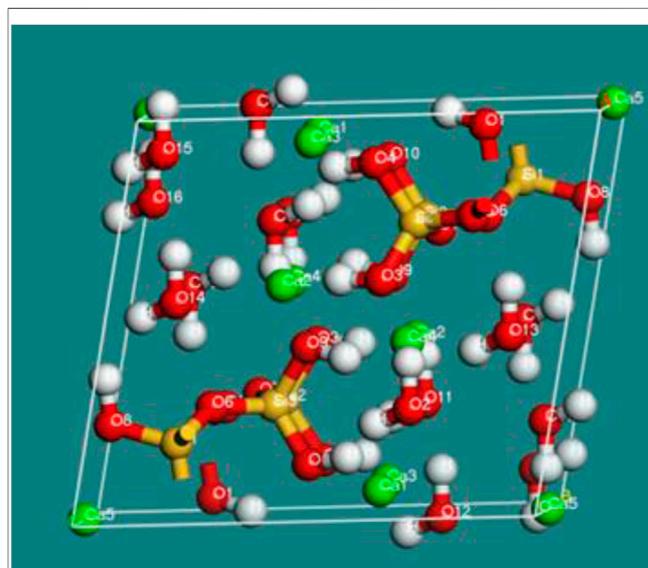
FIGURE 3 | Model of the jennite structure.

orbital at approximately −20 to −16 eV, while the *p* orbitals were mainly attributed to the bonding atomic orbitals at nearly −12 and −7.5 to 0 eV, etc., with the peak value of 41.9 electrons/eV for the density of states before adsorption.

As shown in **Figures 2B,C** some new characteristic peaks of the *p* orbital were present at nearly −12.5 eV. Also rearrangement of the density for the *s* and *p* orbitals, with the peak value (43.2 electrons/eV), was higher than that before the adsorption, which may confirm the chemical bonding and interaction between illite and sodium tartrate. The peak value of montmorillonite (46.5

TABLE 5 | Calculation results for the total energy of jennite after geometry optimization.

Composition	Total energy after geometric optimization/Ha
Jennite (020) surface	−4,796.2470029
Jennite (001) surface	−10,270.6417208
Jennite (010) surface	−10,270.3770792

TABLE 6 | Calculations of the adsorption energy between the different admixtures and jennite.
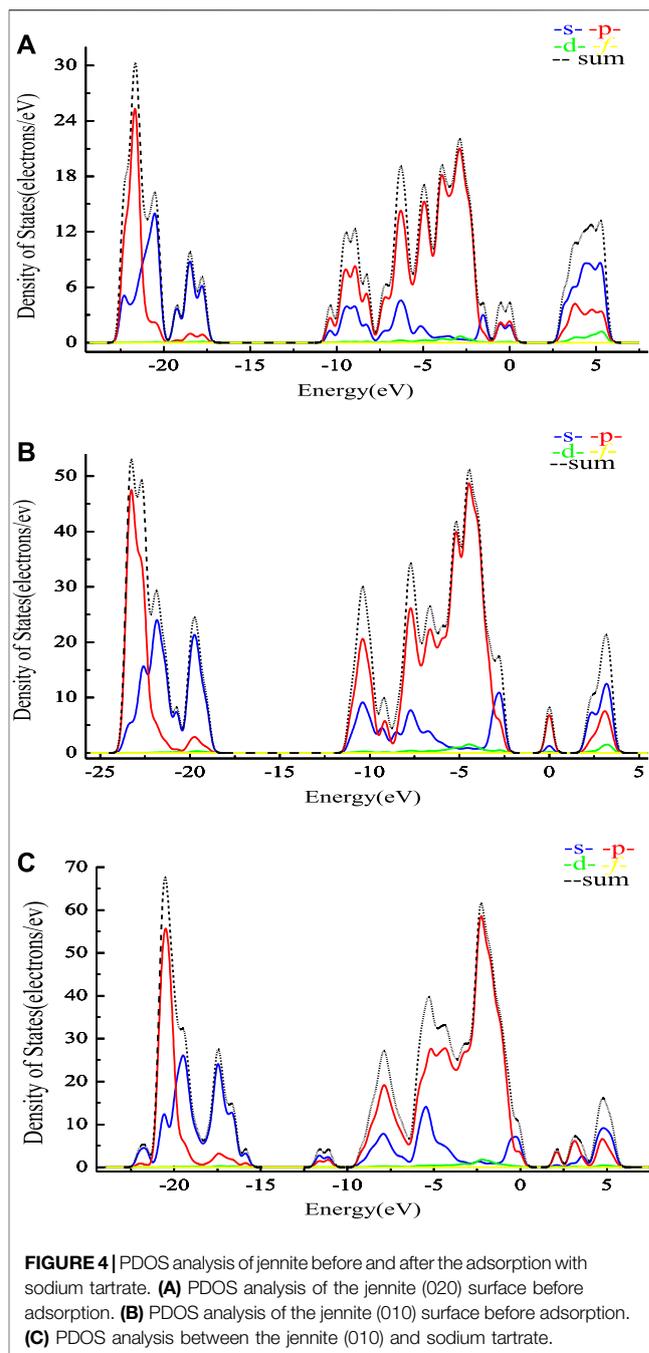
Functional group		E_{ads}/eV
	Jennite (001) surface	2.6964
	Jennite (010) surface	−0.3711
	Jennite (020) surface	0.01614
	Jennite (001) surface	**0.6498**
	Jennite (010) surface	**−8.5237**
	Jennite (020) surface	**−7.6280**
	Jennite (001) surface	4.1260
	Jennite (010) surface	−3.8899
	Jennite (020) surface	−4.6673
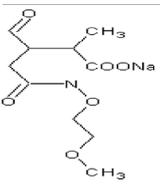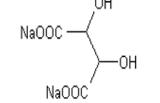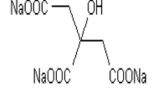
electrons/eV) is also higher than that of illite, which is consistent with the adsorption energy calculated before.

3.2 Adsorption Models of Different Admixtures on Montmorillonite

Based on our previous studies, as montmorillonite has the lowest adsorption energy when compared with the other minerals in bentonite, we will then further compare the adsorption energy between montmorillonite and other typical functional groups shown in **Table 2**, and the calculation result of the adsorption energy is presented in **Table 4**.

There was a large discrepancy in the adsorption energy between different admixtures and montmorillonite. For functional groups such as carboxyl (-COO⁻) (**Table 4a**) and sulfonic acid groups (-SO₃⁻) (**Table 4c**), the adsorption energy has a positive value, suggesting that adsorption for montmorillonite may be rather difficult on additives. The adsorption energy in sodium tartrate is the least among all additives, followed by sodium citrate, indicating that such additives could be easier adsorbed with clay minerals, thus may be more liable to reduce the dispersion of the water reducer in the hydration process. Compared with our previous findings, the adsorption energy of admixtures on montmorillonite clay was usually higher than that on hydration product CH, which demonstrates that admixtures

FIGURE 4 | PDOS analysis of jennite before and after the adsorption with sodium tartrate. **(A)** PDOS analysis of the jennite (020) surface before adsorption. **(B)** PDOS analysis of the jennite (010) surface before adsorption. **(C)** PDOS analysis between the jennite (010) and sodium tartrate.

may be more prone to be adsorbed on CH than clay minerals (He, 2022).

3.3 Adsorption Models Between the C-S-H and Additives
3.3.1 Calculation of Adsorption Energy on C-S-H
Calcium silicate hydrate (C-S-H) may account for a large proportion of all hydration products. As discussed above, we will then take the defined crystal structure of jennite (**Figure 3**) to simulate the C-S-H structure in this text. The calculation results

Atomic layer of sodium tartrate (with atom number)	Mulliken charge populations	
	Before adsorption	After adsorption on the jennite (010) surface
C (1)	0.072	0.084
C (2)	0.353	0.307
C (3)	0.072	−0.285
C (4)	0.353	0.402
O (5)	−0.667	−0.672
O (6)	−0.390	−0.347
O (7)	−0.667	−0.470
O (8)	−0.390	−0.558
O (9)	−0.447	−0.498
O (10)	−0.447	−0.991
H (11)	0.077	0.115
H (12)	0.077	0.178
H (13)	0.245	0.278
H (14)	0.245	0.315
Na (15)	0.707	0.650
Na (16)	0.707	0.647

for the total energy after geometry optimization are shown in **Table 5**.

For the discrepancy of the total energy in different planes of jennite, we will then further build the adsorption models between C-S-H and the above admixtures. The calculation of the adsorption energy is shown in **Table 6**.

The adsorption energy between the jennite (001) surface and different admixtures has positive values, indicating that the adsorption is rather difficult that surface. Jennite (010) and (020) surfaces present a lower adsorption energy in sodium tartrate, indicating that sodium tartrate may be easier to adsorb on the hydration product C-S-H, with a more significant delayed coagulation effect on the hydration reaction. Comparing the adsorption energy of sodium tartrate in clay minerals and hydration products, the adsorption energy of sodium tartrate on hydration product CH is the lowest, followed by montmorillonite, while the adsorption energy of the hydration product C-S-H is the highest (Bonaccorsi et al., 2004; Babaei et al., 2020; Xing et al., 2020).

Combined with the calculation results of adsorption energy between the clay minerals and the hydration products on the admixtures, the binding capacity of bentonite with the admixtures varies due to the difference of mineral composition and the content. The higher the content of montmorillonite, the easier the combination with additives. Also, as the content of CH and C-S-H is not always consistent in different stages of the hydration process, the adsorption energy of admixtures on hydration products would change accordingly. This could also further reflect the preferential adsorption order and compatibility between clay minerals and hydration products on the admixtures.

3.3.2 PDOS of Jennite Before and After the Adsorption

As presented in **Figure 4**, the horizontal axis of the energy for jennite (010) may tend to the lower state when compared with jennite (020). Unlike the minerals as shown in **Figure 2**, the

bonding orbital at approximately −22, −10 ~ −7.5, and 5 eV, etc. may consist of both the *s* and *p* orbitals, while the other peaks of the bonding orbital were mainly provided by a single orbital. The peak value of density of states for jennite (010) (53 electrons/eV) is much higher than that of jennite (020). With higher density of states, the total energy could be higher, which may be positively associated with the total energy of different planes as shown in **Table 4**.

Comparing PDOS before and after adsorption with sodium tartrate, with a higher peak value after adsorption (67.7 electrons/eV), some new characteristic peaks may also occur near −11 and 3 eV. While the extent of change is not so fierce when compared with the minerals as shown in **Figure 2**, which could mean the interaction between jennite is weaker than that of minerals, further confirming the adsorption energy as calculated before.

3.3.3 Mulliken Population Analysis

The distribution of charge between each component atom could be calculated by Mulliken charge populations, which can further provide proof for the bonding and interaction between atoms. Mulliken population analysis for sodium tartrate is presented in **Table 7**.

The charge of the component atoms for sodium tartrate will be varied when adsorbed on jennite, as for the C (3) atom, the Mulliken charge population could change from 0.072 to −0.285, also some of the atoms such as O (7), O (8), O (10), and H (12) would have variable changes. With the variation and redistribution of the electrical charges, we can further intuitively understand the interplay between the additives and hydration product C-S-H.

4 CONCLUSION

This paper mainly analyzes the adsorption characteristic between the hydration product and bentonite clay mineral with additives in the cement hydration process. Combined with the calculation of the adsorption energy and the state density, the competitive adsorption and the compatibility between the hydration product and the clay minerals was further revealed, the conclusions are as follows:

(1) There is competitive adsorption between clay and hydration products when the admixture participates in the hydration reaction. The adsorption sequence of different minerals is as follows: montmorillonite > illite > calcite > orthoclase > quartz. The adsorption energy between the additives and hydration product CH is the lowest, followed by montmorillonite, while the adsorption energy of hydration product C-S-H is the highest.

(2) The binding capacity of bentonite with the admixtures varies due to the difference of mineral composition and the content. The higher the content of montmorillonite, the easier the combination with additives. While the proportions of CH and C-S-H in different stages of the hydration process could also reflect the preferential adsorption order and

compatibility between clay minerals and hydration products on the admixtures.

(3) Comparing PDOS between the minerals and hydration products with different admixtures can also conclude that there are some new characteristic peaks of the p orbital and rearrangement of the density for the s and p orbitals after the adsorption. The peak value of density of states shows a rising trend after adsorption, while the extent of change in jennite is not so fierce when compared with the minerals, which could further verify that the interaction between jennite is weaker than that of minerals.

DATA AVAILABILITY STATEMENT

The datasets presented in this study can be found in online repositories. The names of the repository/repositories and accession number(s) can be found in the article/supplementary material.

REFERENCES

AUTHOR CONTRIBUTIONS

HT contributed for theoretical calculation and thesis writing; ZH and GM contributed for the overall idea and thinking of the manuscript, also the thesis modification; JZ contributed for the processing of data and thesis modification.

Babaei, Z., Najafi Chermahini, A., Dinari, M., and Dinari, M. (2020). Glycerol Adsorption and Mechanism of Dehydration to Acrolein over TiO2 Surface: A Density Functional Theory Study. *J. Colloid Interface Sci.* 563, 1–7. doi:10.1016/j.jcis.2019.12.051

Bao, Li., Liu, S., Guo, J., and Zhang, L. (2018). Interaction Between Low Rank Coal and Kaolinite Particles: A DFT Simulation. *Appl. Surf. Sci.* 456, 215–220. doi:10.1016/j.apsusc.2018.06.121

Bonaccorsi, E., Merlino, S., and Taylor, H. F. W. (2004). The Crystal Structure of Jennite, $Ca_9Si_6O_{18}(OH)_6 \cdot 8H2O$. *Cem. Concr. Res.* 34, 1481–1488. doi:10.1016/j.cemconres.2003.12.033

Chen, J., and Ye, C. (2010). A First-Principle Study of the Effect of Vacancy Defects and Impurity on Adsorption of O_2 on Sphalerite Surface. *Colloids Surf. A:Physiochem Eng. Aspects* 363 (1/3), 56–63. doi:10.1016/j.colsurfa.2010.04.013

Chen, H., Koopal, L. K., Xiong, J., Avena, M., and Tan, W. (2017). Mechanisms of Soil Humic Acid Adsorption onto Montmorillonite and Kaolinite. *J. Colloid Interface Sci.* 504, 457–467. doi:10.1016/j.jcis.2017.05.078

Churakov, S. V. (2008). Hydrogen Bond Connectivity in Jennite from Ab Initio Simulations. *Cem. Concr. Res.* 38, 1359–1364. doi:10.1016/j.cemconres.2008.08.004

Han, H., Rafiq, M. K., Zhou, T., Xu, R., Mašek, O., and Li, X. (2019). A Critical Review of Clay-Based Composites with Enhanced Adsorption Performance for Metal and Organic Pollutants. *J. Hazard. Mater.* 369, 780–796. doi:10.1016/j.jhazmat.2019.02.003

He, Z. (2022). *Study on the Characteristics of Time-Varying Viscosity Grouting Material and its Blocking Mechanism of Tunnel Water Inrush- Take Mira Mountain Section of Linla Highway as an Example*. Chengdu: Chengdu University of Technology. (in Chinese).

Hu, Q. (2013). *Effects of Microfines on the Dispersibility of Polycarboxylate Superplasticizer*. Chongqing: Chongqing University. (in Chinese).

Jae, E. O., Y B, J., and Jeong, Y. (2014). Characterization of Geopolymers from Compositionally and Physically Different Class F Fly Ashes. *Cem. Concr. Compos.* 50, 16–26. doi:10.1016/j.cemconcomp.2013.10.019

Jeffrey, W. B., Hamlin, M. J., and Richard, A. L. (2011). Mechanism of Cement Hydration. *Cem. Concr. Res.* 41, 1208–1223. doi:10.1016/j.cemconres.2010.09.011

Jingming, W., Yang, H., Zhu, J., and Shen, W. (2009). Molecular Dynamic Simulation on Interlayer Micro-structure in Organic Montmorilionite. *J. Mineral. Pet.* 29 (1), 33–37. (in Chinese). doi:10.19719/j.cnki.1001-6872.2009.01.006

Ko, Y. C., and Kang, B. (2016). The Effect of the Mineralogical Composition of Various Bentonites on CEC Values Determined by Three Different Analytical Methods. *Appl. Clay Sci.* 126, 153–159. doi:10.1016/j.clay.2016.03.010

Lei, L., and Plank, J. (2012). Synthesis, Working Mechanism and Effectiveness of a Novel Cycloaliphatic Superplasticizer for Concrete. *Cem. Concr. Res.* 42 (1), 118–123. doi:10.1016/j.cemconres.2011.09.003

Li, C.-Z., Feng, N.-Q., Li, Y.-D., and Chen, R.-J. (2005). Effects of Polyethlene Oxide Chains on the Performance of Polycarboxylate-Type Water-Reducers. *Cem. Concr. Res.* 35 (5), 867–873. doi:10.1016/j.cemconres.2004.04.031

Muralidharan, K., Simmons, J. H., Deymier, P. A., and Runge, K. (2005). Molecular Dynamics Studies of Brittle Fracture in Vitreous Silica: Review and Recent Progress. *J. Non-Crystalline Solids* 351, 1532–1542. doi:10.1016/j.jnoncrysol.2005.03.026

Nathan, A., Tregger, M. E., and Pakula Surendra, P. S. (2010). Influence of Clays on the Rheology of Cement Pastes. *Cem. Concr. Res.* 40, 384–391. doi:10.1016/j.cemconres.2009.11.001

Ng, S., and Plank, J. (2012). Interaction Mechanisms between Na Montmorillonite Clay and MPEG-Based Polycarboxylate Superplasticizers. *Cem. Concr. Res.* 42 (6), 847–854. doi:10.1016/j.cemconres.2012.03.005

Norvell, J. K., Stewart, J. G., Juenger, M. C., and Fowler, D. W. (2007). Influence of Clays and Clay-Sized Particles on Concrete Performance. *J. Mat. Civ. Eng.* 19 (12), 1053–1059. doi:10.1061/(asce)0899-1561(2007)19:12(1053)

Orazi, V., Juan, A., González, E. A., Marchetti, J. M., and Jasen, P. V. (2020). DFT Study of Ethanol Adsorption on CaO(0 0 1) Surface. *Appl. Surf. Sci.* 500, 144254. doi:10.1016/j.apsusc.2019.144254

Pardal, X., Pochard, I., and Nonat, A. (2009). Experimental Study of Si-Al Substitution in Calcium-Silicate-Hydrate (C-S-H) Prepared under Equilibrium Conditions. *Cem. Concr. Res.* 39, 637–643. doi:10.1016/j.cemconres.2009.05.001

Roig-Flores, M., Lucio-Martin, T., Alonso, M. C., and Guerreiro, L. (2021). Evolution of Thermo-Mechanical Properties of Concrete with Calcium Aluminate Cement and Special Aggregates for Energy Storage. *Cem. Concr. Res.* 141, 106323. doi:10.1016/j.cemconres.2020.106323

Sharma, M., Bishnoi, S., Martirena, F., and Scrivener, K. (2021). Limestone Calcined Clay Cement and Concrete: A State-Of-The-Art Review. *Cem. Concr. Res.* 149, 106564. doi:10.1016/j.cemconres.2021.106564

Vidmer, A., Sclauzero, G., and Pasquarello, A. (2014). Infrared Spectra of Jennite and Tobermorite from First-Principles. *Cem. Concr. Res.* 60, 11–23. doi:10.1016/j.cemconres.2014.03.004

Wang, Z., Hu, Q., Wang, Y., Wang, L., and Zhang, L. (2013). Interlayer Absorption Characteristics of Montmorillonite to Polycarboxylate Superplasticizer. *J. Chin. Ceram. Soc.* 41 (8), 1100–1104. (in Chinese). doi:10.7521/j.issn.0454-5648.2013.08.12

Wang, J., Ma, H., Yuan, W., He, W., Wang, S., and You, J. (2014). Synthesis and Characterization of an Inorganic/organic-Modified Bentonite and its Application in Methyl Orange Water Treatment. *Desalination Water Treat.* 52 (40/41/42), 7660–7662. doi:10.1080/19443994.2013.830690

Wang, L. (2013). *Effect of Clay Minerals on the Performance of Polycarboxylate Superplasticizer and Mechanism Research*. Beijing: China University of Mining & Technology. (in Chinese).

Wu, Y., Zhang, L., Liu, Y., and Qu, Y. (2018). Adsorption Mechanisms of Metal Ions on the Potassium Dihydrogen Phosphate (1 0 0) Surface: A Density Functional Theory-Based Investigation. *J. Colloid Interface Sci.* 522, 256–263. doi:10.1016/j.jcis.2018.03.073

Xing, J., Wang, C., Zou, C., and Zhang, Y. (2020). DFT Study of Se and SeO_2 Adsorbed on CaO (0 0 1) Surface: Role of Oxygen. *Appl. Surf. Sci.* 510, 145488. doi:10.1016/j.apsusc.2020.145488

Yan, Y. (2017). *Atomic Simulation and Performance Design of the Calcium Silicate Hydrates*. Nanjing: Southeast University. (in Chinese).

Yinwen, L., Chaolong, Y., Yunfei, Z., Jian, Z., Huilong, G., and Mangeng, L. (2014). Study on Dispersion, Adsorption and Flow Retaining Behaviors of Cement Mortars with TPEG-type Polyether Kind Polycarboxylate Superplasticizers. *Construction and Build. Mater.* 64, 324–332. doi:10.1016/j.conbuildmat.2014.04.050

Zhang, J., Pei, X., Wang, W., and He, Z. (2017). Hydration Process and Rheological Properties of Cementitious Grouting Material. *Constr. Build. Mater.* 139, 221–231. doi:10.1016/j.conbuildmat.2017.01.111

Zhang, S., Liu, Q., Gao, F., Li, X., Liu, C., Li, H., et al. (2017). Mechanism Associated with Kaolinite Intercalation with Urea: Combination of Infrared Spectroscopy and Molecular Dynamics Simulation Studies. *J. Phys. Chem. C.* 121 (1), 402–409. doi:10.1021/acs.jpcc.6b10533

Zhang, Y, Kong, X, Lu, Z, and Hou, S (2015). Effects of the Charge Characteristics of Polycarboxylate Superplasticizers on the Adsorption and the Retardation in Cement Pastes. *Cement and Concrete Res.* 67, 184–196. doi:10.1016/j.cemconres.2014.10.004

Zhang, Y., He, Z., Tian, H., Huang, X., Zhang, Z., Liu, Y., et al. (2021a). Hydrochemistry Appraisal, Quality Assessment and Health Risk Evaluation of Shallow Groundwater in the Mianyang Area of Sichuan Basin, Southwestern China. *Environ. Earth Sci.* 80 (17), 576. doi:10.1007/s12665-021-09894-y

Zhang, Y., Dai, Y., Wang, Y., HuangXiao, X. Y., Xiao, Y., and Pei, Q. (2021b). Hydrochemistry, Quality and Potential Health Risk Appraisal of Nitrate Enriched Groundwater in the Nanchong Area, Southwestern China. *Sci. Total Environ.* 784, 147186. doi:10.1016/j.scitotenv.2021.147186